Oscillatory neck propagation in polymer films: 2

Akihiko Toda
Department of Physics, Faculty of Science, Kyoto University, Kyoto 606, Japan
(Received 5 November 1993; revised 8 February 1994)

The oscillatory behaviour of neck propagation during cold drawing of polymer films has been studied numerically. Previous calculations based on Barenblatt's model considering the temperature rise at the neck have been refined by introducing heat diffusion and the consequent temperature distribution in the film. Period doubling of the oscillation and other phenomena that were observed experimentally and remained to be explained have been produced by the refined model.

(Keywords: neck propagation; self-excited oscillation; period doubling)

INTRODUCTION

The plastic deformation of polymer materials often starts from a localized deformation, so-called necking, and is followed by the propagation of the neck.

Neck propagation such as that of amorphous poly(ethylene terephthalate) (PET) films sometimes shows the following unusual behaviours. Under the condition of constant drawing rate, the propagation becomes unstable within a certain range of drawing rates, and the required stress and the velocity of neck propagation begin to oscillate (*Figures 1* and *2*)[1]. By constant-load drawing, the velocity of neck propagation shows discontinuities and hysteresis ('a' and 'c' in *Figure 3*), missing the velocity range of oscillatory neck propagation observed under constant drawing rate ('b' in *Figure 2*)[2,3].

In a previous paper[4], the oscillation and the stability of neck propagation were studied on the basis of Barenblatt's model[5], describing neck propagation as a non-isothermal process. Before introducing Barenblatt's model, we briefly review oscillatory neck propagation in the following.

Oscillatory neck propagation

The oscillating behaviour is mainly observed in the region of $d\sigma/dV<0$ on a plot of required stress σ against drawing rate V (*Figure 2*), i.e. the region where the required stress becomes smaller as the drawing rate increases. It is noted that, even in this region, neck propagation is stable in the early stage of drawing (*Figure 1*).

During the oscillation at constant drawing rate, the following occurs repeatedly: elastic deformation of the transformed and untransformed parts of the sample with almost zero velocity of neck propagation and then quick propagation of the neck with elastic shrinkage of those transformed and untransformed parts. This means that the elastic deformation of the sample is coupled with a certain mechanism of neck propagation.

The period of oscillation becomes longer with the progress of drawing; the period is determined by the elastic compliance of the whole system, which is an increasing function of the total length of the sample.

The amplitude of oscillation changes with drawing rate and becomes smaller as the rate increases (*Figure 2*).

Concerning the temperature rise considered in Barenblatt's model, it is experimentally confirmed that the surface temperature at the neck rises up to 95°C[6]. On the other hand, if the sample is immersed in a liquid, wrapped by an aluminium foil or blown to remove the heat produced by the work of drawing at the neck, the oscillation disappears. Under such a condition, the plot of stress vs. logarithm of drawing rate shifts upwards ('d' in *Figure 2*) and lies on a straight line extrapolated from the values at slow drawing rates ('a' in *Figure 2*); the linear dependence of σ on log V indicates a kinetics controlled by the rate process of Eyring[7].

Barenblatt's model

Barenblatt's model regards the process of neck propagation as a non-isothermal process caused by a temperature rise at the neck. The process comprises a dynamical system in a phase space of σ, v and T. The oscillatory neck propagation is explained as a self-excited oscillation expressed by a limit cycle in the phase space.

In the model, the relationship between stress σ and velocity v is assumed to be dependent only upon the temperature T at the neck and hence the physical state of neck propagation is expressed by those three parameters. The relationship between those parameters is represented by a function:

$$f(\sigma, v, T)=0 \tag{1}$$

which gives the physically allowed set of variables σ, v and T located on a surface in three-dimensional space (σ, v, T). The simplest form of function will be given by

0032-3861/94/17/3638-05

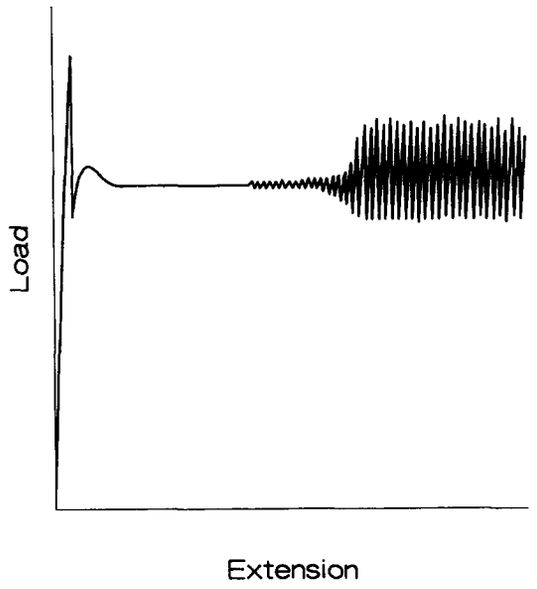

Figure 1 Typical load–extension curve of oscillatory neck propagation

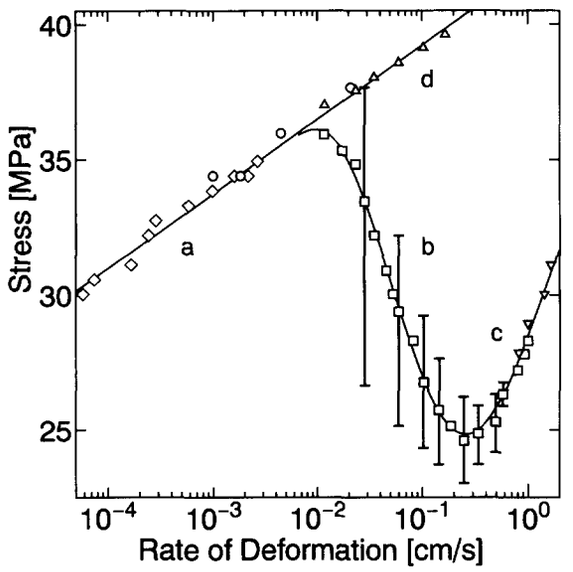

Figure 2 Plots of stress against deformation rate obtained experimentally[4]. The PET films are 300 μm thick and 3 mm wide. Drawing conditions: (◇) constant load in air; (○) constant load in water; (△) constant speed in water; (□) constant speed in air; (▽) constant load in air. The bars represent the amplitude of stress oscillation

Eyring's rate process[7]:

$$v = v_0 \exp\left(-\frac{\Delta F}{kT}\right)\left[\exp\left(\frac{\alpha\sigma}{kT}\right) - \exp\left(-\frac{\alpha\sigma}{kT}\right)\right] \quad (2)$$

where ΔF and α are the activation free energy and volume for the process and k is the Boltzmann constant.

On the other hand, the following equation gives the heat balance at the neck:

$$\rho C_p \omega \frac{dT}{dt} + \rho C_p S_1 v(T - T_0) = -\beta S(T - T_0) + S_1 \sigma v \quad (3)$$

where T_0 represents the ambient temperature, ρ and C_p the density and specific heat of the material, β the heat-transfer coefficient, S_1 the original cross-sectional area of the sample, and ω and S the volume and surface area of the neck region. The second term on the left-hand side of equation (3) represents the heat removed from the neck region by the propagation of the neck. The first term on the right-hand side represents the heat transferred from the neck region to the surroundings, and the last term gives the heat produced by the work done at the neck per unit time[4].

The stationary solution of equations (2) and (3) ($dT/dt = 0$) gives σ, v and T of steady neck propagation (*Figure 4*). The curve shown in *Figure 4* actually reproduces the N-shaped dependence of stress on drawing rate[4].

For drawing at constant speed V, the process must satisfy the following additional condition:

$$v + \lambda \, d\sigma/dt = V \quad (4)$$

where λ is the elastic compliance of the whole system,

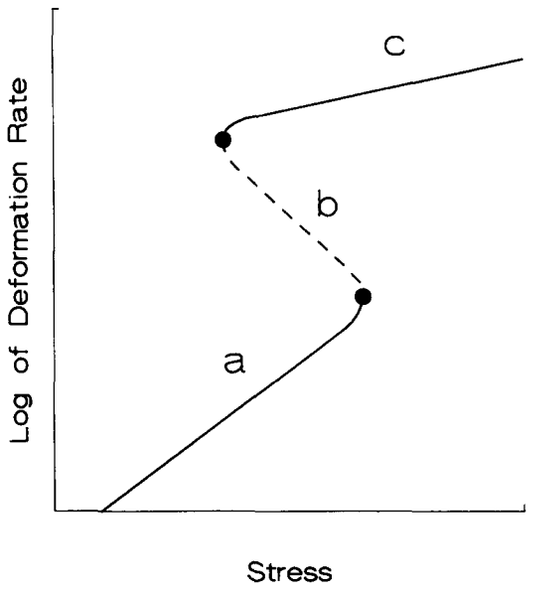

Figure 3 Schematic plot of deformation rate vs. stress for drawing at constant load[3]

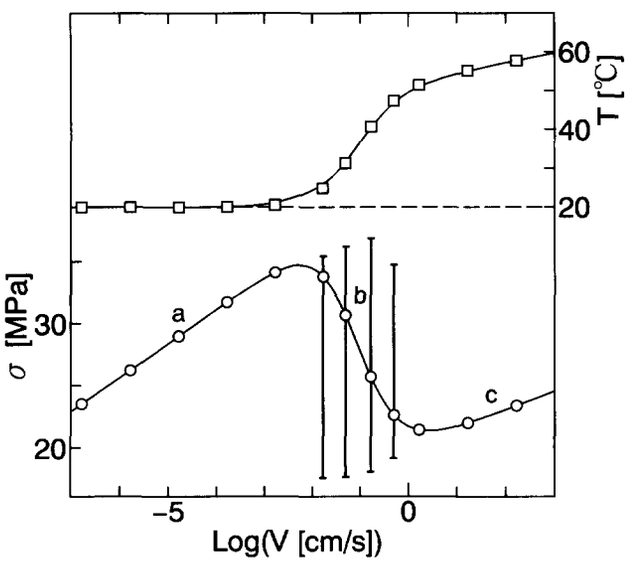

Figure 4 Plots of the stationary solutions of equations 2), (3) and (4)[4]. The bars represent the amplitude of stress oscillation

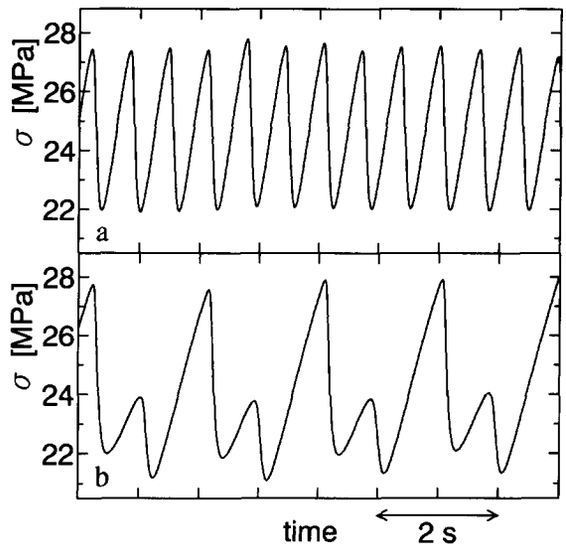

Figure 5 Typical oscillatory behaviour in stress observed experimentally. The PET films are 1 mm thick and 3 mm wide. The early stage of stress oscillation is shown in (a) and the later one in (b). The change in the period and the occurrence of period doubling are clearly seen

which gradually becomes large as the sample becomes elongated but, in the time interval of several periods of oscillation, can be regarded as a constant parameter because λ increases very slowly with the elongation of the sample[5]. The stress σ in this equation is the apparent stress, namely $\sigma = P/S_1$, where P is the applied load. Equation (4) means that the rate of total deformation is given by the sum of the rates of neck propagation, v, and the elastic deformation of the sample, $\lambda\, d\sigma/dt$.

By numerical calculations of the differential equations (2), (3) and (4), it has been confirmed that the steady-state solution shown in *Figure 4* becomes unstable in the region 'b' of *Figure 4* ($d\sigma/dV < 0$) for λ larger than a critical value λ_c, namely at the later stage of neck propagation, and then oscillatory neck propagation appears[4].

Unsolved questions

Several important features of oscillatory neck propagation still remain unexplained by Barenblatt's original model[5] and the numerical calculations[4]:

(i) In *Figure 4*, the amplitude of stress oscillation obtained from the numerical calculations is shown against drawing rate. The amplitude was almost independent of the drawing rate and hence equations (2), (3) and (4) did not reproduce the experimentally observed dependence of amplitude on drawing rate (bars in *Figure 2*).

(ii) As shown in *Figure 2*, stress oscillation appears not only in the region 'b' ($d\sigma/dV < 0$) but also in 'c'. However, the detailed analysis of equations (2), (3) and (4) showed that neck propagation in the region of $d\sigma/dV > 0$ must be stable[4].

(iii) At the later stage of drawing, the period of oscillation sometimes becomes doubled, as shown in *Figure 5*. Such a period doubling cannot be expected from the dynamical system of equations (2), (3) and (4), where the number of independent variables is only two[8].

(iv) Calculation results shown in *Figure 4* could not reproduce the sharp rise in stress against drawing rate in the region 'c' of *Figure 2*.

The objective of the present paper is to investigate possible solutions to the above difficulties in the original Barenblatt model[5] and the detailed analysis[4]. Instead of equation (3) considering the temperature rise only at the neck, we utilize the following thermal diffusion equation:

$$\rho C_p \frac{dT}{dt} + \rho C_p v \frac{dT}{dx} = -h\left(\frac{1}{a}+\frac{1}{b}\right)(T - T_0) + k\frac{d^2T}{dx^2} + \frac{S_1}{\omega}\sigma v \quad \text{for } 0 \leqslant x \leqslant \Delta x \text{ in the neck region} \quad (5)$$

considering the distribution of temperature, $T(x, t)$, in the sample. In equation (5), the x axis is taken along the elongation direction of the sample with the origin fixed at the neck, k and h represent the thermal conductivity of the material and the heat transfer coefficient of the surrounding air, and a and b are the width and thickness of the sample. In the neck region ($0 \leqslant x \leqslant \Delta x$), we add the contribution of the heat production by the work of drawing, $S_1 \sigma v/\omega$.

NUMERICAL CALCULATION

We try to obtain the numerical solutions to equations (2), (4) and (5). Employing equation (2) means that the relationship between stress, neck propagation velocity and temperature is expressed by Eyring's rate process (equation (2)). Such a dependence is seen experimentally[2,4] and will provide a reasonable dependence between them.

For the parameters in equation (2), we use the same values as those in the previous paper[4]: $v_0 = 2.25 \times 10^{72}$ cm s^{-1}, $\Delta F = 8.17 \times 10^{-12}$ erg and $\alpha = 3.39 \times 10^{-21}$ cm^3. The following values of the physical parameters in equation (5) were taken from the literature[9]: $\rho = 1.34$ g cm^{-3}, $C_p = 1.12 \times 10^7$ erg g^{-1} K^{-1}, $k = 1.50 \times 10^4$ erg cm^{-1} s^{-1} K^{-1} and $h = 2.33 \times 10^3$ erg cm^{-2} s^{-1} K^{-1}. Concerning the size of sample, a, b and S_1 ($\equiv ab$), used in equation (5), those values were taken from the experimental values as $a = 0.3$ cm and $b = 0.1$ cm; the dimensions of the sample are not typical of those in the experiments, but with such thick films self-oscillation occurs more easily.

We utilize a finite difference method to solve equations (2), (4) and (5). The mesh size, Δx, is fixed at 0.005 cm. The length of the neck region was assumed to be equal to the single mesh size. The volume of the neck region is expressed by the mesh size as $\omega = \Delta x S_1$; in the present calculations, we neglect the change in the size of sample by deformation at the neck, as we will discuss later. This choice of the volume of the neck region has an influence on the degree of temperature rise at the neck because the heat production term (the last term) in equation (5) is divided by the volume, ω. In order to raise the temperature to 60°C ($T_0 = 20$°C) at high drawing rates (*Figure 9*), this term is multiplied by a factor 2.5 in the following calculations.

We choose the explicit (Euler forward) scheme of the finite difference method and make the following restrictions on the values of Δt in order to assure the consistency of the scheme: $\Delta t \leqslant 0.05(\Delta x)^2/\kappa$, $\Delta t \leqslant 0.05\,\Delta x/v(t)$ and $0.99 \leqslant v(t+\Delta t)/v(t) \leqslant 1.01$, where κ ($\equiv k/\rho C_p$) represents the thermal diffusivity. The last condition is required because the neck propagation velocity changes exponentially during the oscillation

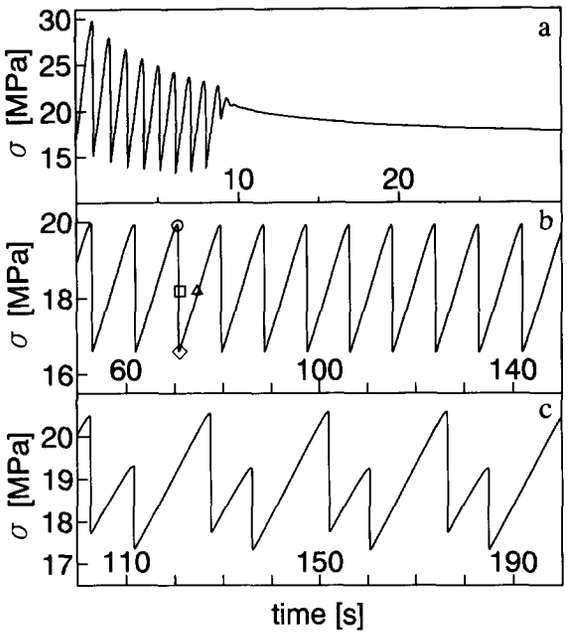

Figure 6 Plots of calculated σ as a function of time for drawing at constant speed. The rate of drawing is 0.014 cm s^{-1}. The parameter λ takes the values of 0.001, 0.03 and 0.06 cm MPa^{-1} for (a), (b) and (c) respectively

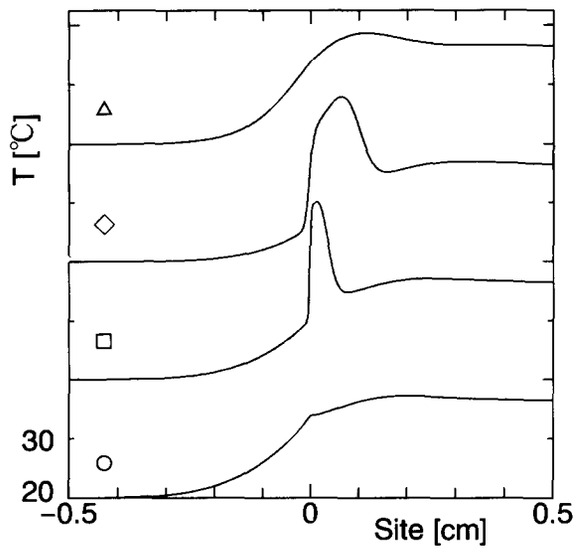

Figure 7 Calculated temperature profile along the elongation direction during oscillation at the time denoted by ○, □, ◇ and △ in *Figure 6b*

process. In order to approximate the term representing the thermal convection, $v\,dT/dx$, in equation (5), we mainly take the first-order upwinding method; with a higher-order approximation of third-order upwinding, there were no essential differences in the behaviours. The number of meshes was taken to be sufficiently large not to affect the results: in most cases, $-150\Delta x \leqslant x \leqslant 300\Delta x$.

In each calculation, the compliance of the system, λ, was fixed because of its slow variation during the actual drawing process. We examine the development of neck propagation, namely the change in σ, v and T, for different λ and V by solving equations (2), (4) and (5) numerically.

RESULTS

The following results were obtained from the numerical calculations of equations (2), (4) and (5) for drawing at constant velocity.

Figure 6 shows the change in stress with time for different values of λ. For small λ (*Figure 6a*), the neck propagation is stable and the stress oscillation due to an initial disturbance is relaxed to the steady state. For sufficiently large λ (*Figure 6b*), stable oscillation appears. *Figure 7* shows the temperature distribution in the sample at the time indicated by the symbols on the curve in *Figure 6b*. For still larger λ (*Figure 6c*), the period doubling of oscillation can be seen. *Figure 8* shows the changes in T, v and σ during the oscillation with double period. *Figure 9* shows the plots of stress and temperature

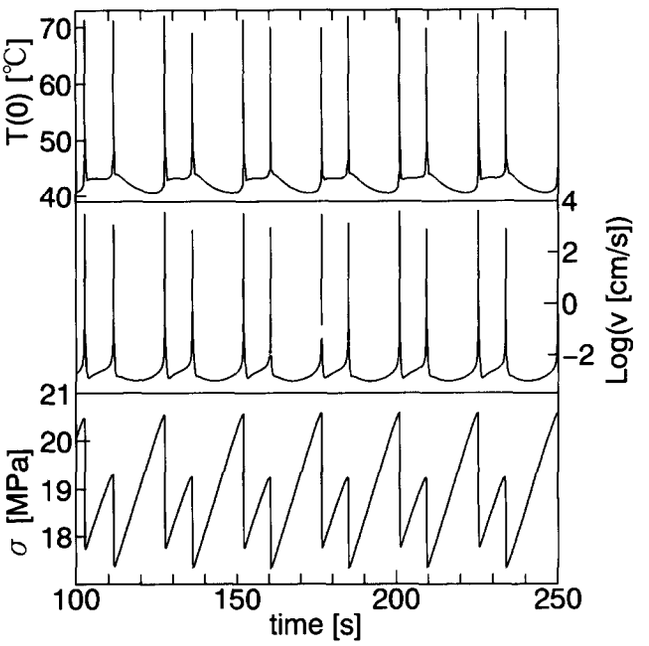

Figure 8 Plots of calculated σ, $\log v$ and T as functions of time. The rate of drawing is 0.014 cm s^{-1} and the parameter λ is 0.06 cm MPa^{-1}: the same condition as in *Figure 6c*

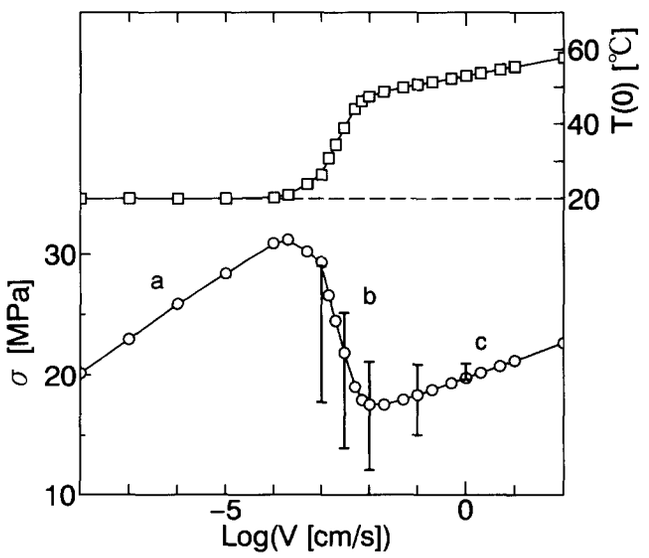

Figure 9 Plots of the stationary solutions to equations (2), (4) and (5). The bars represent the amplitude of stress oscillation

against drawing velocity under steady state, namely for λ small enough to ensure stable neck propagation.

DISCUSSION

Concerning the unsolved questions given in the above, we could have reproduced the experimental results pointed out in questions (i)–(iii) by the present numerical calculations of the differential equations (2), (4) and (5).

(i) Amplitude of stress oscillation was dependent on drawing rate (*Figure 9*).

(ii) Stress oscillation appeared in the region of $d\sigma/dV > 0$, namely 'c' in *Figure 9*.

(iii) Period doubling of stress oscillation occurred for large λ ('c' in *Figure 6*).

In the present numerical calculations, we have utilized the thermal diffusion equation (5) instead of equation (3), considering the temperature rise only at the neck region. Owing to the diffusion, the heat produced at the neck is conducted to the untransformed region and raises the temperature there (*Figure 7*). This temperature rise will be responsible for the above results, which are different from the previous ones obtained from equation (3).

Regarding the steep rise in stress against drawing velocity in the region 'c' of *Figure 2*, such a strong dependence could not be reproduced by the present calculations (*Figure 9*). It is possible that Eyring's rate process employed in the present calculations, equation (2), is not applicable to neck propagation at high temperatures. But it is more probable that the temperature at the neck has been lowered as the drawing rate becomes faster in the region 'c' of *Figure 2* due to the fast removal of the produced heat from the neck region by its fast propagation. The experimentally observed steep rise in stress in the region 'c' of *Figure 2* might have been caused by this effect, though such a decrease in temperature did not occur in the present calculations. We need experimental and theoretical investigations on this point.

It is a well known fact that crystallization of amorphous PET films follows necking at high drawing rates during the oscillation[1]. It was postulated that crystallization makes an essential contribution to the occurrence of hysteresis and oscillation[2]. But crystallization actually occurs after deformation apart from the neck region[10] and hence it will be a subsidiary effect of the temperature rise caused by drawing. For simplicity, we have neglected the effect of crystallization in the present calculations, though crystallization might have some influence on the process as an additional heat source.

Lastly, it should be noted that the differential equation (5) used in the present calculations does not fully correspond to the actual neck propagation process. In the actual process, neck propagation is followed by elongation of the sample and shrinkage of the cross-sectional area, namely the elongation of the positive x axis and the change in a and b in the equation. We have taken the present form of the differential equation (5) because of its simplicity. Since we have not yet understood the condition for the occurrence of period doubling in the oscillation, we needed to reduce the number of controlling parameters in the calculations.

Probably, because of the simplification, the resultant period of oscillation (*Figure 6*) became much longer than the experimental period (*Figure 5*). The period of self-oscillation is determined not only by the compliance but also by the drawing rate. It can be said that the period becomes longer by slowing down the drawing rate, though the analytical expression of the oscillation period has not been obtained. In the present calculation, we have utilized the physical constants of the actual PET film, but the range of drawing rate, in which oscillation occurs, was lower than the previous one by more than one order of magnitude: region 'b' in *Figures 4* and *9*. The slow drawing rates in the region 'b' of *Figure 9* are directly responsible for the long oscillation period obtained in the present numerical calculations. Here, lowering the range 'b' is due to the temperature rise at the neck for slower drawing rates in the present model than in the previous one. This could be due to the simplification in the model, as mentioned above. But since the heat removed from the neck region is stored in the necked and unnecked part of the sample in the present calculation (*Figure 7*), it is also probable that the removed heat contributes to the temperature rise at the neck region; such an effect has been neglected in Barenblatt's original model.

For those reasons, we should consider the success of the present analysis in a restricted sense. Irrespective of such a restriction, the basic feature of the present analysis provides a reasonable explanation of the process and will remain correct. We certainly need further refinements to the model.

ACKNOWLEDGEMENT

This work was partly supported by a Grant-in-Aid for Scientific Research from the Ministry of Education, Science and Culture of Japan.

REFERENCES

1 Andrianova, G. P., Kechekyan, A. S. and Kargin, V. A. *J. Polym. Sci. (A-2)* 1971, **9**, 1919
2 Pakula, T. and Fischer, E. W. *J. Polym. Sci., Polym. Phys. Edn* 1981, **19**, 1705
3 Yamane, T., Umemoto, S., Okui, N. and Sakai, T. *Polym. Prep. Japan* 1991, **40**, 1284
4 Toda, A. *Polymer* 1993, **34**, 2306
5 Barenblatt, G. I. *Mech. Solids* 1970, **5**, 110
6 Roseen, R. *J. Mater. Sci.* 1974, **9**, 929
7 Ward, I. M. 'Mechanical Properties of Solid Polymers', Wiley, New York, 1971, Ch. 11
8 Haken, H. 'Advanced Synergetics', Springer-Verlag, Berlin, 1983, Ch. 1
9 Lawton, E. L. and Ringwald, E. L. 'Polymer Handbook' (Eds J. Brandrup and E. H. Immergut), Wiley, New York, 1989, p. V-101
10 Toda, A. unpublished work